CNWRA 2003-04
Revision 1

ANALYSIS OF RAIL CAR COMPONENTS EXPOSED TO A TUNNEL FIRE ENVIRONMENT

Prepared for

U.S. Nuclear Regulatory Commission
Contract NRC–02–02–012

Center for Nuclear Waste Regulatory Analyses
San Antonio, Texas

CNWRA 2003-04
Revision 1

ANALYSIS OF RAIL CAR COMPONENTS EXPOSED TO A TUNNEL FIRE ENVIRONMENT

Prepared for

U.S. Nuclear Regulatory Commission
Contract NRC–02–02–012

Prepared by

Andre S. Garabedian
Darrell S. Dunn
Asadul H. Chowdhury

Center for Nuclear Waste Regulatory Analyses
San Antonio, Texas

November 2002

ABSTRACT

Rail car components recovered from the train involved in the July 18, 2001, Howard Street Tunnel, Baltimore, Maryland train derailment and fire were used to estimate the fire duration and temperatures achieved by the components. Steel samples including sections of the box car panels and a bolt from an air brake assembly were analyzed using standard metallurgical methods to determine oxide layer thickness and the amount of metal lost as a result of the elevated temperature exposure. Aluminum alloy air brake valve assemblies, which melted as a consequence of the fire, were analyzed using a heat transfer model.

Analyses of the recovered components suggest the surface temperature of the steel reached 700 to 850 °C [1,292 to 1,562 °F] assuming an exposure time of 4 hours at the elevated temperatures. Independent assessment of fire duration could not be obtained from the steel components because the oxide scale thickness and metal loss are dependent on both time and temperature. Several limitations to the assessment of temperature were noted including the effects of oxide-scale spalling and post-fire atmospheric exposure for a period of more than 1 year.

Thermal analysis of the aluminum air brake valve body located approximately 10 m [33 ft] from the fire (at the brake end of Car 52) indicated melting occurred early in the fire event, and the temperature achieved by this component was at least 600 °C [1,112 °F]. A similar aluminum cover located at approximately 20 m [66 ft] from the fire (at the mid-point of Car 51) was only partially melted indicating its temperature may have reached 600 °C [1,112 °F] for a limited time, where an aluminum cover located approximately 30 m [98 ft] away from the spill site (at the brake end of Car 53) was not affected by the fire exposure at all. This temperature profile indicating a decrease in exposure temperature with distance away from the spill site was further substantiated by the lack of damage to other components, such as railcar exterior paint.

The analyses conducted suggest the temperatures achieved by materials present in a confined space fire are strongly dependent on the proximity of the component of interest to the fire source. Gas temperatures near the fire source were likely in excess of 800 °C [1,472 °F] for more than 30 minutes and the reaction of components in this region were likely influenced by the direct radiation from the fire. At a distance of approximately 20 m [66 ft] from the fuel source, where the dominant mode of heat transfer was convection, the exposure was capable of generating surface temperatures as high as 600 °C [1,112 °F], however, only for a much shorter duration.

CONTENTS

FIGURES

ACKNOWLEDGMENTS

This report was prepared to document work performed by the Center for Nuclear Waste Regulatory Analyses (CNWRA) for the U.S. Nuclear Regulatory Commission (NRC) under Contract No. NRC–02–02–012. The activities reported here were performed on behalf of the NRC Office of Nuclear Material Safety and Safeguards, Spent Fuel Project Office. The report is an independent product of the CNWRA and does not necessarily reflect the views or regulatory position of the NRC.

The authors thank Yi-Ming Pan and Jason Huczek at Southwest Research Institute® for their technical assistance provided at various stages of the project. The authors thank Yi-Ming Pan, Jason Huczek, and B. Sagar for their technical and programmatic reviews of this report and C. Cudd and A. Woods for editorial reviews. The authors are thankful to C. Patton for assisting with the word processing and preparation of the report.

QUALITY OF DATA, ANALYSES, AND CODE DEVELOPMENT

DATA: No CNWRA-generated original data are contained in this report. Sources for other data should be consulted for determining the level of quality for those data.

ANALYSES AND CODES: Spreadsheet calculations were accomplished using Microsoft® Excel 2000. Analyses are documented in Scientific Notebook 550.

1 BACKGROUND

On July 18, 2001, a 60-car train, carrying flammable liquids, corrosive acids, paper products, and other commodities derailed while passing through the Howard Street Tunnel in Baltimore, Maryland. This incident derailed 11 cars, Cars 46 through 56, while on an upward slope of approximately 0.8 percent.

The derailment caused structural damage to Car 52, carrying approximately 106,000 L [28,000 gal] tripropylene, puncturing the base of the tank and initiating a fuel spill. A fire ensued, which burned freely for 3 hours. After approximately 3 hours into the event, a water main ruptured above the tunnel, introducing cooling water to the tunnel.

On August 27, 2002, the U.S. Nuclear Regulatory Commission (NRC) directed the Center for Nuclear Waste Regulatory Analyses to support the NRC and the National Transportation Safety Board in Washington, DC, to review and analyze the information obtained from the site visit of the stored, fire damaged cars from the Baltimore tunnel accident. Information obtained from the site visit and specimens from the rail cars were analyzed to estimate the duration of exposure and temperatures achieved by the fire-damaged cars. The objectives and scope of work discussed in this report are based on this directive.

2 OBJECTIVES AND SCOPE OF WORK

The goal of the project was to compile forensic evidence about the materials damaged during the tunnel fire and to use engineering methods to gain insight into the thermal environment the materials experienced during the fire. An estimation of the thermal environment at approximately 20 m [66 ft] on each side of the fire source will also be provided.

The thermal environment is defined by a temperature-time history. Two analyses needed to be conducted to establish this history:

Establish a Rough Temperature Achieved by Samples—Determine the rough-temperature profile by analyzing the phase change in materials collected from the site. These data will indicate the maximum temperatures achieved and may give a rough estimation of the duration. The source of such data is the metallurgical analysis of the exposed steel and aluminum components in the vicinity of the fire.

Predict the Duration—Correlate the rough-temperature history gained by metallurgical analysis to physical observations (e.g., melting). Using heat transfer equations and the metallurgical estimation of temperature, the predicted thermal environment can be imposed on the sample to determine whether damage, consistent with the damage observed, could have been caused by the exposure. In this case, the predictor will be the total phase change (melting) of a die-cast aluminum cover plate.

The analysis will focus on the vicinity of the tripropylene car before the water introduction because the thermal environment conditions are assumed to have been the worst. Analyses of the fire environment were directed, specifically, to the fire environment surrounding three air brake valve assemblies in the vicinity of the spilled tripropylene.

The prediction of the thermal environment in the vicinity of the air brake valve served to provide a better estimate for the thermal environment in the zones of interest {15–20 m [49.21–65.62 ft] to either side of a presumed spill site}. Data in the vicinity of the air brake valves will be extrapolated to other zones of interest, because there was no readily observable evidence of the thermal environment in these areas (e.g., no distinct melting, charring, or obvious deformation).

3 SAMPLES COLLECTED TO DATE

Several samples were collected from the site. Samples were chosen because of their proximity to the fire source and their level of damage.

These materials included

Steel Scale, Taken from the Brake End of Car 51—This location was adjacent to the brake end of Car 52 and was approximately 10–12 m [32.81–39.37 ft] uphill from the fire source.

Section of Roof Plate from Car 50—The steel section was taken from the roof of Car 50 because this location was the source of a substantial, secondary fire as a result of the prolonged paper fire.

Remainder of ABDX-L Air Brake Valve from Car 52—This air brake valve exhibited evidence of prolonged fire exposure. The valve includes several die-cast aluminum covers, which had completely melted as a result of the fire. The valve was found approximately 10 m [33 ft] uphill from the spill site, and approximately 1 m [3.3 ft] from the tunnel floor. A similar valve assembly was found at the midpoint of Car 51, approximately 20 m [66 ft] uphill from the fire source. Although the exact model type was not determined, the valve cover was clearly from the same family of products and was composed of the same aluminum alloy. A third air brake valve was found approximately 30 m [100 ft] from the spill site, and analyzed.

Exposed Bolts Remaining on Air Brake Valve Assembly—The bolts used to hold the die-cast aluminum covers were retrieved for subsequent analysis.

Sand Sample Adhered to the Base of Rail #44—Rail #44 (as identified by National Transportation Safety Board) was in the vicinity of the derailment and the fire source. The sand sample was taken from the south face of the track. The sand was of interest because it had exhibited some form of phase change, which transformed it from a powder to a consolidated mass.

New ABDX-L Air Brake Valve Cover and Attaching Bolts—A new valve cover and mounting hardware were provided by the manufacturer, WABTEC. These components were collected with the intent of defining a baseline for subsequent metallurgical analyses. Neither the aluminum cover nor the bolts were fully analyzed as part of this project because these samples were not received in time to be included in this report.

3.1 Valve Assembly

The valve assembly found on Car 52 was identified as an ABDX-L valve. The valve assembly located on Car 51 was also assumed to be an ABD valve assembly. A complete ABDX-L valve assembly is shown in Figure 3-1.

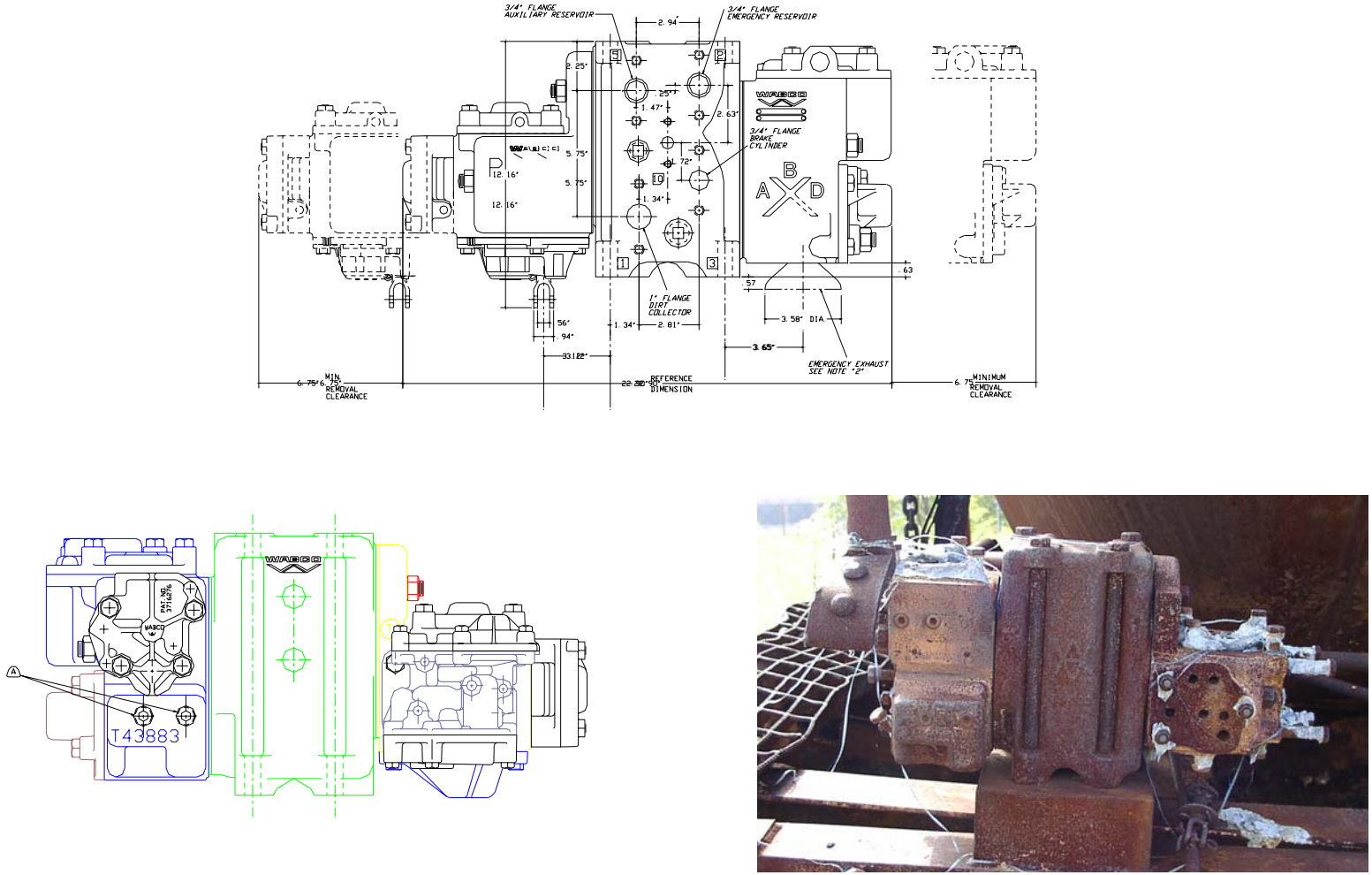

Figure 3-1. The ABDX-L Control Valve (Clockwise from Top: Valve Body Schematic, Photograph of Damaged Valve on Car 52, Corresponding Outline of the Valve Body)

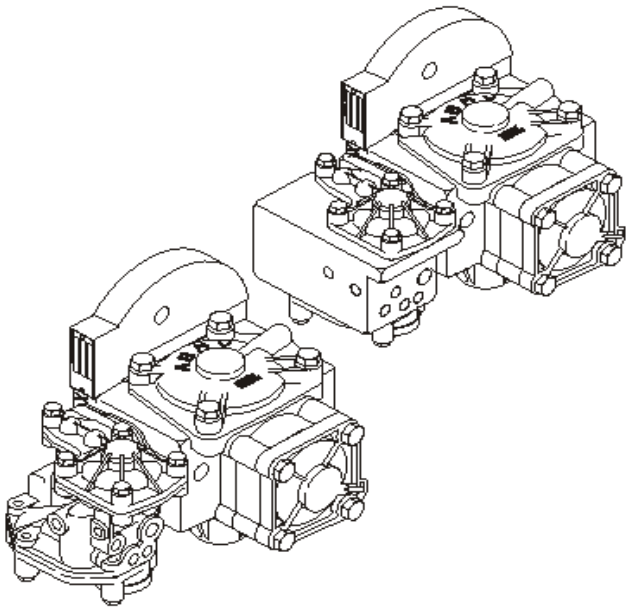

Figure 3-2. ABDX-L Service Portion Outline and Photograph

The standard ABDX-L-style valve consists of a normal service valve and an emergency valve. For this analysis, the damage observed on the service portion of the valve was analyzed (see Figure 3-2).

The primary area of interest in the analysis was the aluminum alloy cover over the release valve in the service portion of the valve assembly shown in Figure 3-2. The location of the cover is marked by the four bolts remaining on one side of the valve, and the associated aluminum residue.

The following assumptions were made regarding the aluminum component based on observations made during the site visit and photographic documentation of the rail cars after the accident:

Material:	Die-Cast Aluminum Alloy (ASTM B 85-99 Grade 360, aluminum-silicon alloy)
Dimensions[1]*:*	127 mm [5 in] diameter, 25.4 mm [1 in] thick
Heat Transfer Area:	Circumference and one side 228 cm² [35 in²]
Volume:	Assuming full depth of 322 cm³ [20 in³]
Orientation:	Vertical

3.2 Valve Materials

As stated by the manufacturer, the aluminum cover plate is composed of ASTM B 85-99 Alloy 360. It is assumed that the alloy is an aluminum-silicon alloy, the properties for which are common for a range of alloy percentages. The alloy has the following properties (Holman, 1990):

Thermal Conductivity (k):	177 W/m K
Density (ρ):	2,707 kg/m³
Specific Heat:	0.892 kJ/kg K
Melting Temperature:	600 ˚C [873 K]

3.3 Steel Samples

Samples were taken from Car 51 (scale), the air brake valve of Car 52 (bolt shown in Figure 3-2) and the roof of Car 50. Samples from the roof panel of Car 50 and the bolt from the airbrake valve of Car 52 were cut from their respective pieces using a low-speed saw. Care was taken not to disturb or heat the oxide scales on these samples.

3.4 Sand Samples

Samples of sand were taken from the Howard Street Tunnel away from the proximity of the fire as well as sand that was adhered to the base of Rail #44.

[1]Dimensions scaled from WABTEC Drawing. 0592776,000,00

4 METALLURGICAL ANALYSES

Metallurgical analyses were performed on each of the samples described in Section 3. The analytical methods were selected to identify the phases present, determine the composition of the phases, and where appropriate, measure important dimensions of the components. Observed properties were compared to published properties for each of the materials, and an estimate of the thermal conditions required to produce these phase changes was derived.

4.1 Analysis Method

Sand samples collected from the Howard Street Tunnel and oxides on the steel specimens were analyzed using x-ray diffraction and Raman spectroscopy. In addition, specimens were mounted in epoxy and cross sectioned for metallurgical analyses. The cross-sectioned specimens were examined using both an optical microscope and a scanning electron microscope with an energy dispersive spectrometer.

Estimations of component temperature and fire duration were made by assessing the extent of iron oxidation and metal loss. Oxidation of iron and carbon steels is dependent on temperature. At temperatures as high as 1,600 °C [2,912 °F], both magnetite (Fe_3O_4) and hematite (α–Fe_2O_3) are stable (Rapp, 1980). Wustite ($Fe_{1-y}O$) is stable in the temperature range of 567 to 1,400 °C [1,052 to 2,552 °F]. Wustite formed at elevated temperatures is not stable at lower temperatures and is transformed to Fe + Fe_3O_4. The rate of oxidation is also dependent on temperature. At a temperature of 250 °C [482 °F] or greater, the oxide on iron and steels grows at a parabolic rate (Szlarska-Smialowska and Jurek, 1976; Runk and Kim, 1970). The thickness of the oxide scale, X, is a function of time according to Eq. (4-1)

$$X^2 = k_p t \qquad (4\text{-}1)$$

where k_p is the rate constant and t is time. A similar expression can be used to determine the metal recession rate as a consequence of oxidation (Simms and Little, 1987).

Figure 4-1 shows the rate constants for metal reduction (k_r), and scale thickness (k_p) obtained for an Fe-$2^1/_4$Cr-1Mo steel and iron. Rate constants for Fe-$2^1/_4$Cr-1Mo were reported by Simms and Little (1987) and Larose and Rapp (1997) over a temperature range from 550 to 700 °C [1,022 to 1,292 °F]. Kubaschewski and Hopkins (1962) reported rate constants for iron from 500 to 1,100 °C [932 to 2,012 °F]. The composition and microstructure of the steels are known to affect oxidation kinetics. Additions of carbon increases the oxidation kinetics of steel. Oxidation kinetics are faster for fine pearlite compared to coarse pearlite or a spheroidized microstructure (Runk and Kim, 1970). Based on data published by Kubaschewski and Hopkins, (1962) , the reduction in metal thickness as a consequence of oxidation under isothermal conditions is shown in Figure 4-2. The change in the rate of metal loss as a function of time is a result of oxide spalling. Similarly, the metal oxide thickness as a function of time and temperature can be calculated and is shown in Figure 4-3. It should be noted that the calculated values for reduction in metal thickness and oxide scale thickness shown in Figures 4-2 and 4-3 do not consider the effects of composition because the calculations are based on results observed for iron. The effect of microstructure was also not considered (Runk and Kim, 1970). Oxide cracking and spalling are assumed when the oxide scale is greater than 85 µm in thickness (Simms and Little, 1987;(Kubaschewski and Hopkins, 1962). Error in the assessment of temperature as a consequence of neglecting compositional and microstructural effects

should be considered. Increasing the carbon content of steel from 0.2 to 0.8 wt% increases the rate constant for oxide film thickness by 42 percent (Runk and Kim, 1970). Microstructure has similar effect. Runk and Kim (1970) reported the rate constant for 0.81 wt% carbon steel with a fine pearlite structure to be 52 percent greater than that for a spheroidized microstructure. Oxide film spalling is known to occur at temperatures as low as 700 °C [1,292 °F] (Kubaschewski and Hopkins, 1962). Spalling results in exposure of the underlying metal and, as a result, can significantly increase the rate of metal loss. Metal loss and oxide scale thickness shown in Figures 4-2 and 4-3 are calculated assuming that the oxidation kinetics after scale spalling are identical to a clean metal surface. It should be noted that the calculated oxide scale thickness shown in Figure 4-3 is the total oxide scale thickness which considers the change in oxidation rate as a result of spalling. The observed scale is likely to be much thinner as a consequence of sloughing after cracking and spalling.

Additional metallurgical analyses of the undamaged steel components may have been useful to assess the temperature and time of exposure. To perform these analyses, corresponding components that were not exposed to elevated temperatures are needed to assess the effects of the fire temperature and duration on microstructural changes. Because the corresponding components were not available for comparison, however, these analyses were not performed.

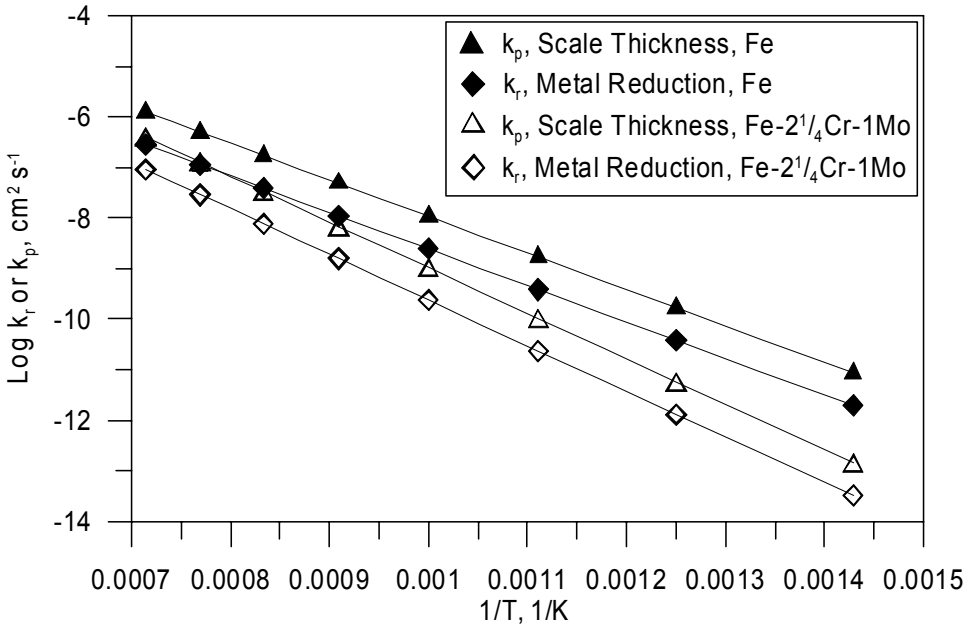

Figure 4-1. Oxidation Rate Constants for Fe-2¼Cr-1Mo Steel and Iron as a Function of Temperature (Simms and Little, 1987; Kubaschewski and Hopkins, 1962)

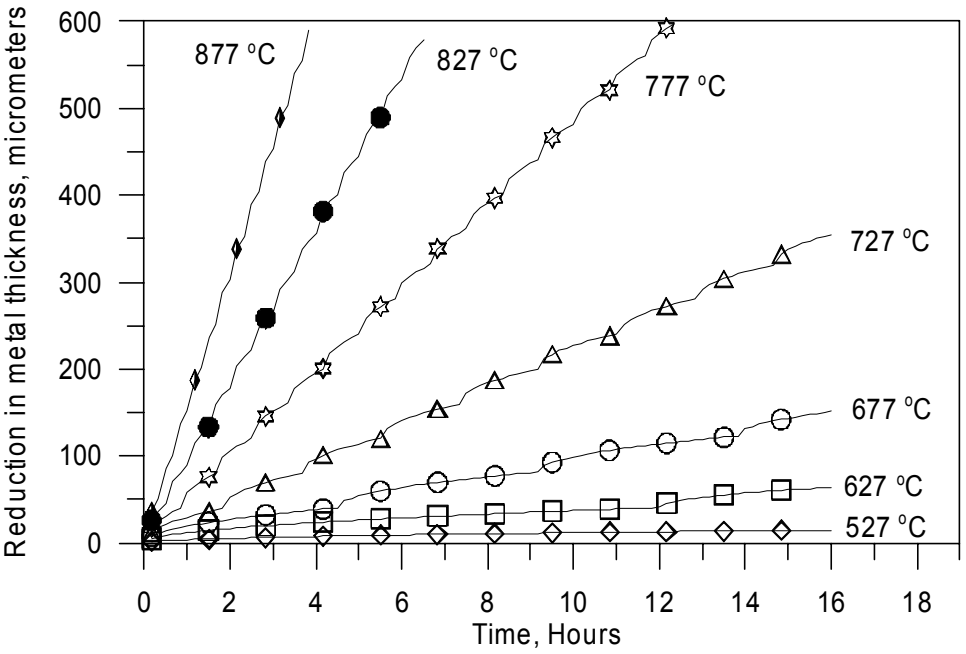

Figure 4-2. Reduction in Metal Thickness as a Function of Time for Isothermal Exposures of Iron in the Range of 527 to 877 °C [980 to 1,610 °F]

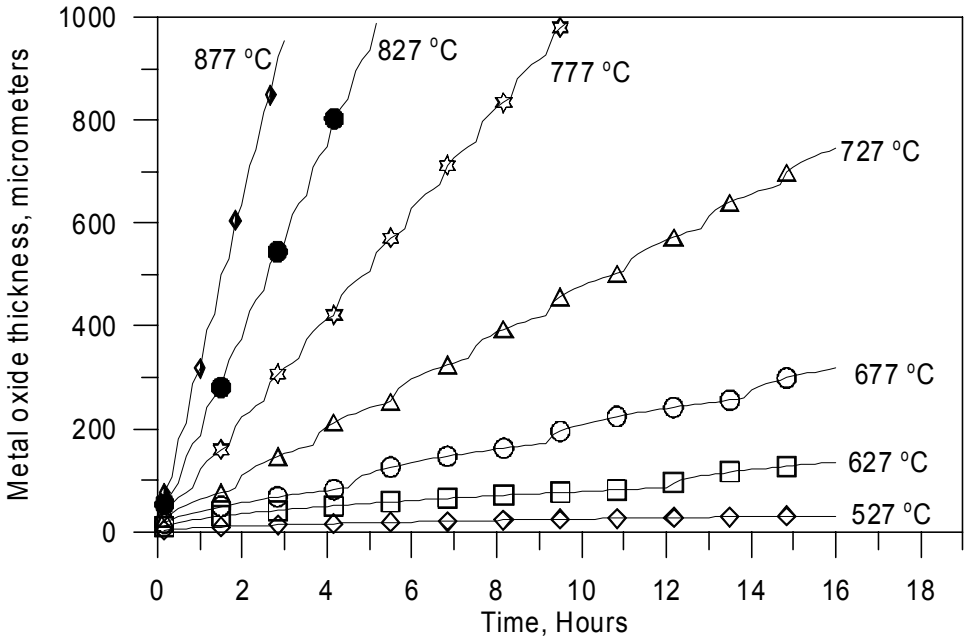

Figure 4-3. Metal Oxide Thickness as a Function of Time for Isothermal Exposures of Iron at Temperatures Ranging from 527 to 877 °C [980 to 1,610 °F]

4.2 Results

Both Raman spectroscopy (Figure 4-4) and x-ray diffraction (Figures 4-5 and 4-6) of the scale obtained from Car 51 indicate the presence of leproidocrocite (γ–FeOOH), hematite (α–Fe_2O_3) and possibly magnetite (Fe_3O_4). It should be noted that magnetite can easily be oxidized in air to hematite. The presence of γ–FeOOH, which covered large sections of the scales, indicates that the specimens were exposed to either a humid environment or water. Formation of γ–FeOOH may have occurred as a result of water contact after rupture of the water main, fire fighting efforts, or subsequent storage of the train cars involved in the derailment.

As indicated in Section 4.1, the thickness of the iron oxide scale is a function of temperature and time. Although thickness of the scales obtained from Car 51 varied, a thickness of 400 to 430 µm [0.016 to 0.017 in] was obtained by examination of the specimen cross section. Initial calculations using Eq. (4-1) and rate constants from Kubaschewski and Hopkins (1962) show that an oxide of 420 µm [0.017 in] can be formed at 777 °C [1,430 °F] in 4 hours. At 827 °C [1,520 °F], a 420-µm [0.017 in] thick scale can be produced in 2 hours.

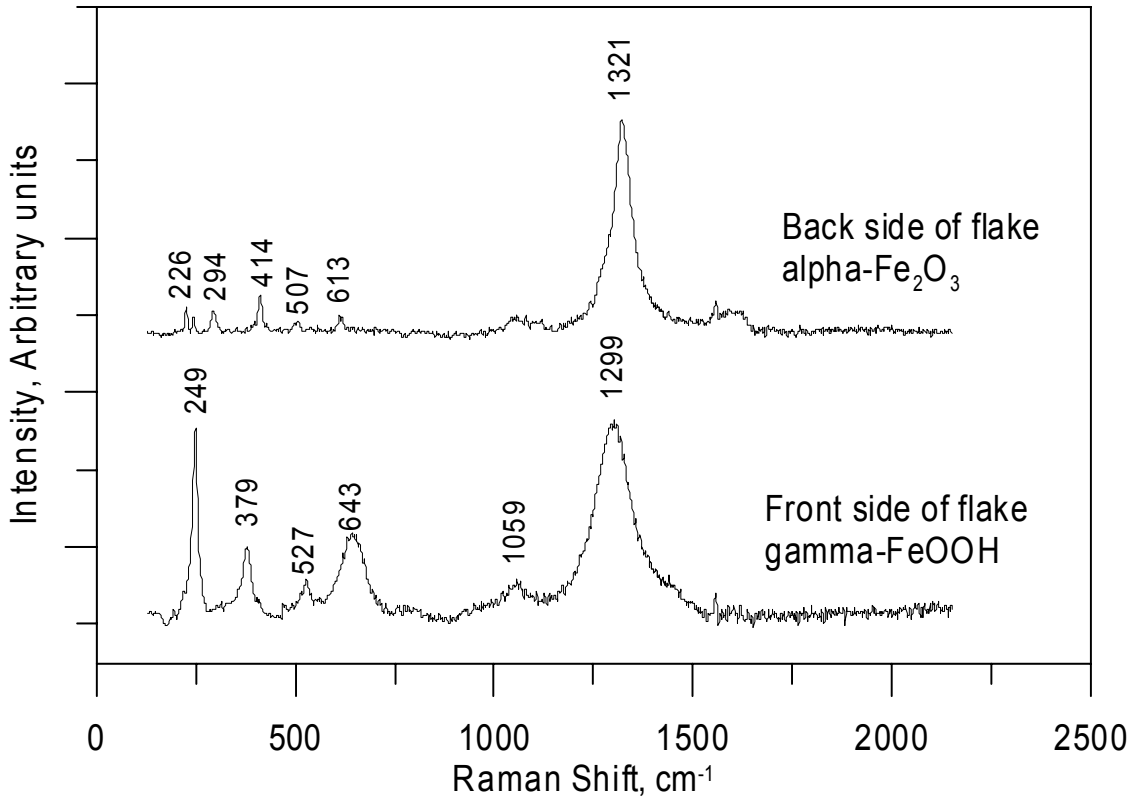

Figure 4-4. Raman Spectra for Scales Recovered from Car 51

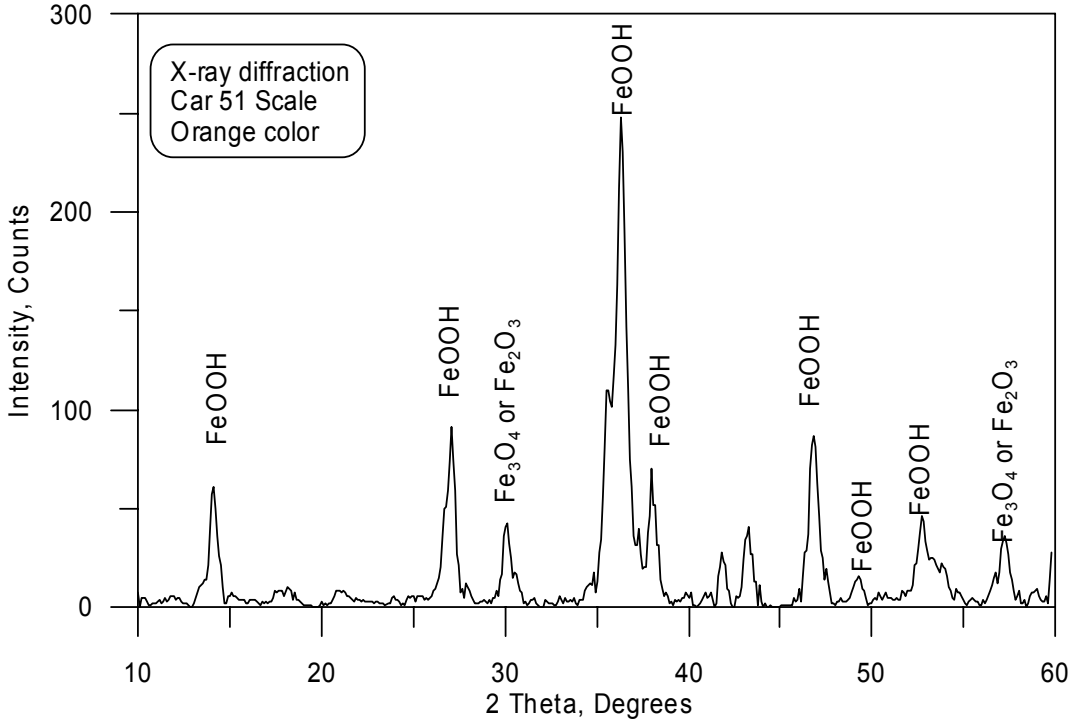

Figure 4-5. X-Ray Diffraction of Orange Colored Oxide Scales from Car 51

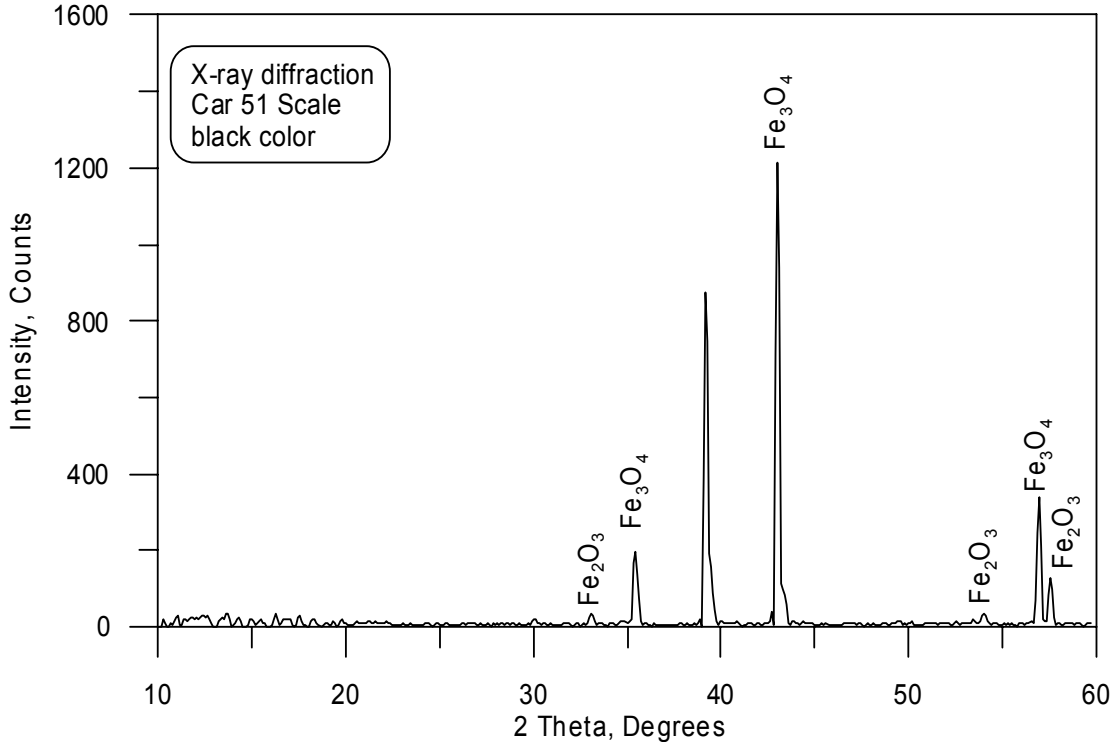

Figure 4-6. X-Ray Diffraction of Black Colored Oxide Scales from Car 51

Specimens from the roof section of Car 50 were analyzed for oxide scale thickness as well as the thickness of the remaining steel section. The first specimen was cut from the opposite end of the roof panel section that may not have been directly exposed to the fire (Figure 4-7). The second specimen was cut from the edge of the roof panel section that was directly exposed to flames from the paper inside the box car (Figures 4-8 and 4-9). From the cross section of the roof shown in Figure 4-7, the remaining metal thickness was determined to be 1,761 µm [0.069 in]. Near the edge of the roof, the metal thickness varies from 829 µm [0.033 in] at the edge (Figure 4-9), to 1,464 µm [0.058 in] at a distance approximately 3 cm [1.2 in] from the exposed edge (Figure 4-8). Although it is apparent that the metal thickness of the roof section shown in Figure 4-7 has been reduced by oxidation, the metal thickness of this section was used as a basis to determine metal loss. Assuming that metal loss occurred at equal rates on both sides of the specimen shown in Figures 4-8 and 4-9, the metal loss from each side varied from 148 to 466 µm [0.006 to 0.018 in]. Based on the calculated reduction in metal thickness as a function of time and temperature shown in Figure 4-2, temperatures in the range of 750 to 850 °C [1,382 to 1,562 °F] for approximately 4 hours would be required to achieve the reduced metal thickness.

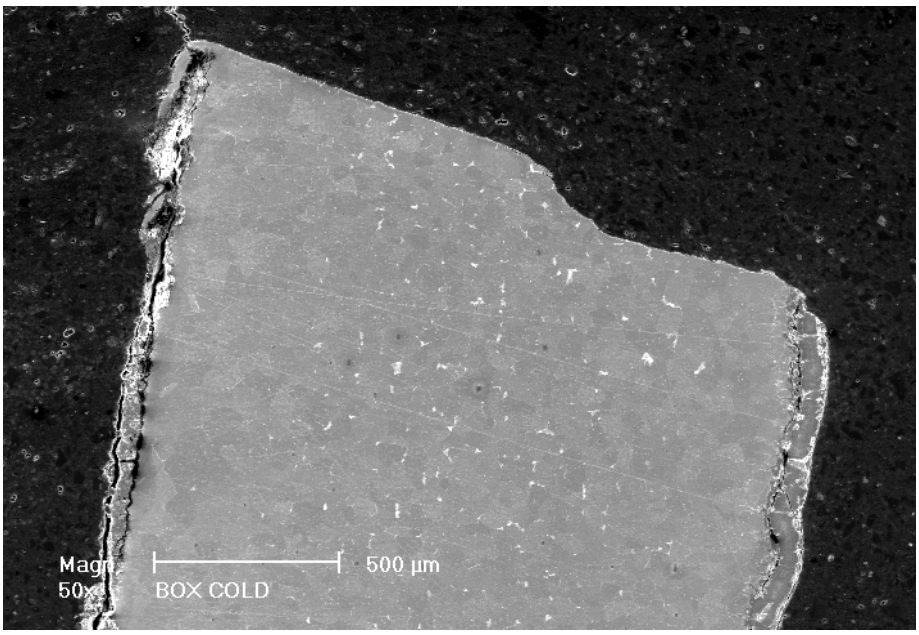

Figure 4-7. Cross section of Car 50 Roof Approximately 40 cm [16 in] from the Opposite End of the Roof Panel Section that May Not Have Been Exposed to the Fire. Thickness of the Metal was Approximately 1,761 µm [0.069 in].

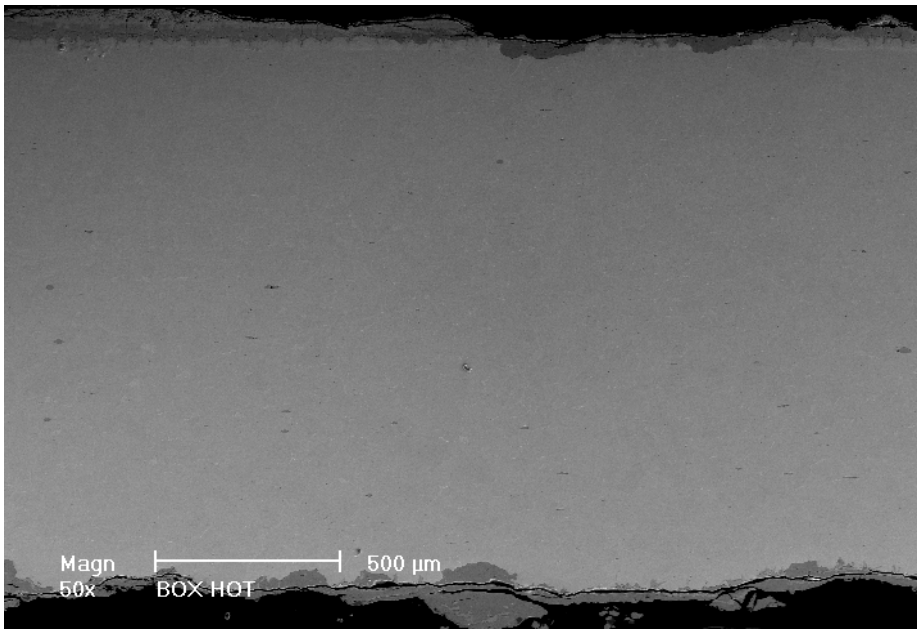

Figure 4-8. Cross Section of Car 50 Roof Approximately 3 cm [1.2 in] from the Edge Directly Exposed to the Fire. Thickness of the Metal was Approximately 1,464 µm [0.057 in].

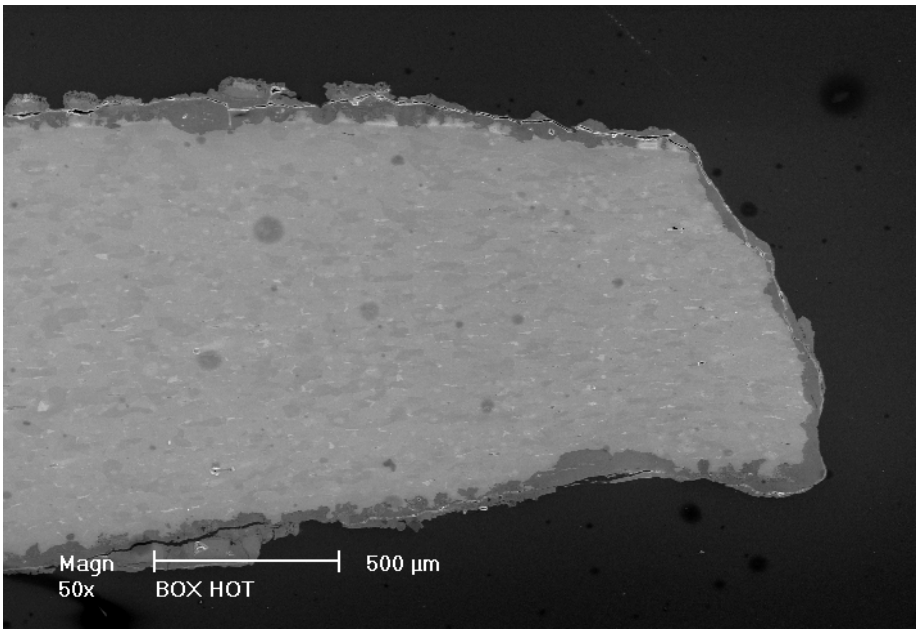

Figure 4-9. Cross Section of Car 50 Roof at Edge Directly Exposed to the Fire. Thickness of the Metal Ranged from 829 to 930 µm [0.033 to 0.037 in].

Figure 4-10(a) shows a closeup of the metal oxide scale of the Car 50 roof section near the edge exposed to the fire. Cracks and spalling of the oxide are apparent from the cross section. Figure 4-10(b) shows the scanning electron microscope-energy dispersive spectrometer element map for iron, and Figure 4-10(c) shows the element map for oxygen which confirms the scale is an iron oxide. Based on the analyses of the cross-sectioned specimen, the oxide scale on the roof section exposed to the fire ranged from 50 to 81 µm [0.0019 to 0.0032 in] in thickness. According to the calculations shown in Figure 4-3 scales of this thickness can be produced at temperatures below 700 °C [1,292 °F] for a period of 4 hours. However, the oxide scale shown in Figure 4-10(a) has clear signs of spalling which may have reduced the scale thickness that remained attached to the damaged roof section.

The cross section of the air brake bolt is shown in Figure 4-11. The oxide scale on the bolt shank was determined to be 53 µm [0.0021 in]. Little spalling or cracking of the oxide layer was observed, suggesting the temperature was less than that achieved by the roof panel of Car 50. Based on the predicted metal oxide thickness shown in Figure 4-3, a 53 µm [0.0021 in] oxide scale could be expected in 4 hours at 627 °C [1,160 °F]. At higher temperatures, spalling of the oxide would be expected.

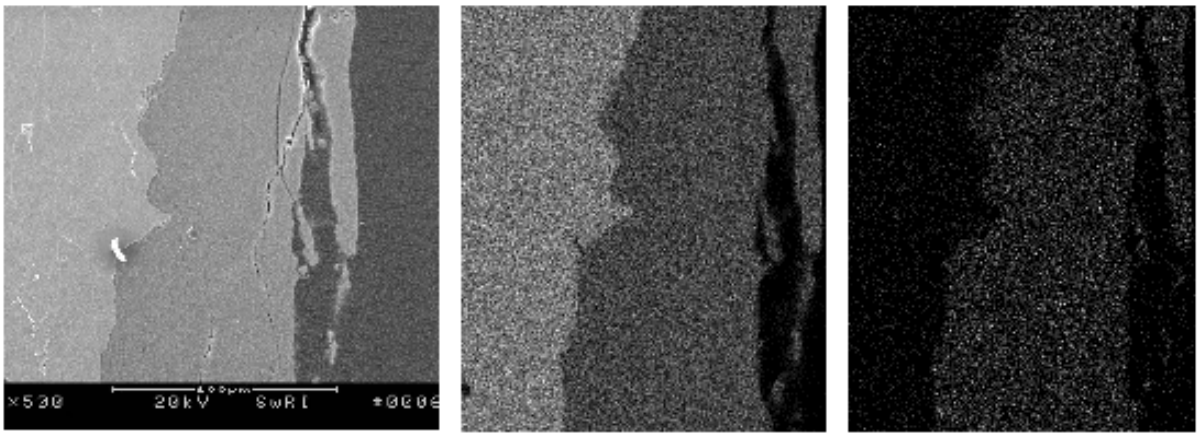

Figure 4-10. (a) Secondary Electron Image from Car 50 Roof at Edge Directly Exposed to the Fire, (b) Iron Image Map, (c) Oxygen Image Map

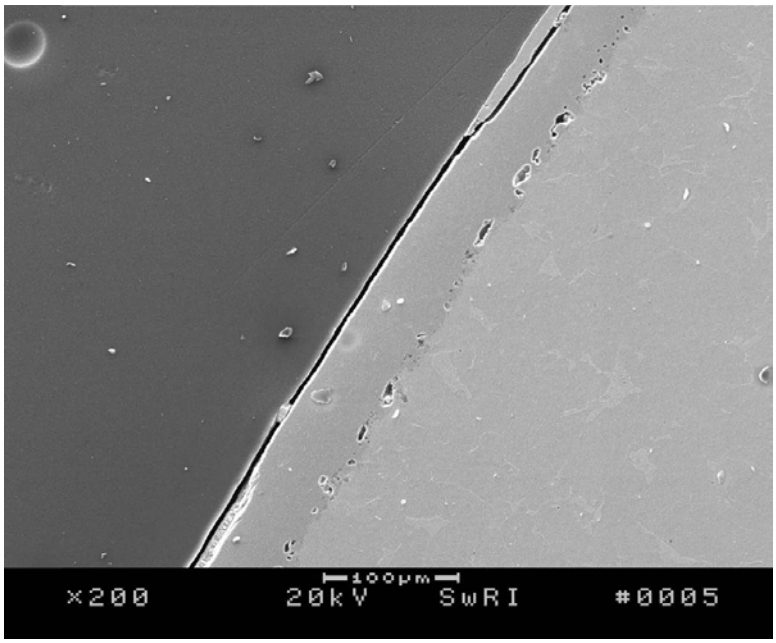

Figure 4-11. Scanning Electron Microscope Secondary Electron Image of Car 52 Air Brake Valve Bolt Showing Metal and Oxide Layer

Figure 4-12(a) shows a cross section of one of the air brake assembly bolts. During the analysis of the specimen, several regions were found where an aluminum–iron phase had formed. A higher magnification of such a region is shown in Figure 4-12(b). Using an energy dispersive spectrometer, the composition of the bolt was determined to be 98.4 atomic percent iron with no measurable concentration of aluminum. In the mixed aluminum–iron region, the composition was found to be 66 atomic percent aluminum, 4 atomic percent silicon, and 30 atomic percent iron. The liquidus temperature for a 66 atomic percent Aluminum and 34 atomic percent iron binary is 1,180 °C [2,156 °F] and the solidus temperature is 1,165 °C [2,129 °F] (ASM International, 1992). The aluminum–iron binary phase diagram does not contain low melting point eutectic compositions. The addition of 4 atomic percent silicon is not expected to significantly alter the solidus or liquidus temperatures based on examination of the iron–silicon and aluminum–silicon binary systems.

The aluminum–iron phase identified on the air brake valve bolt may have been formed as a result of diffusion of aluminum into the iron at elevated temperatures. Eq. (4-2) describes simple diffusion

$$x = \sqrt{Dt} \tag{4-2}$$

where x is the diffusion distance (cm) [in], D is the diffusion coefficient ($cm^2\ s^{-1}$) [$in^2\ s^{-1}$] and t is time (seconds). Assuming a diffusion distance of 100 µm [0.0039 in] and a time of 10 hours, the calculated value of D is 2.8×10^{-9} $cm^2\ s^{-1}$ [4.3×10^{-10} $in^2\ s^{-1}$]. The value of D is dependent on temperature. For face center cubic iron (γ-Fe), a self-diffusion coefficient of 2.8×10^{-9} $cm^2\ s^{-1}$ [4.3×10^{-10} $in^2\ s^{-1}$] corresponds to a temperature of 1,464 °C [2,667 °F] (Geiger and Poirier, 1980).

The sand samples were identified as quartz (SiO_2) using Raman spectroscopy. Results of x-ray diffraction analyses also indicated quartz and small amounts of ankerite [$Ca(Fe,Mg)(CO_3)_2$]. The sample obtained from Rail #44 also had Raman peaks consistent with the presence of γ–FeOOH. As previously indicated, the presence of γ–FeOOH is consistent with corrosion of iron and steel rather than oxidation at elevated temperatures.

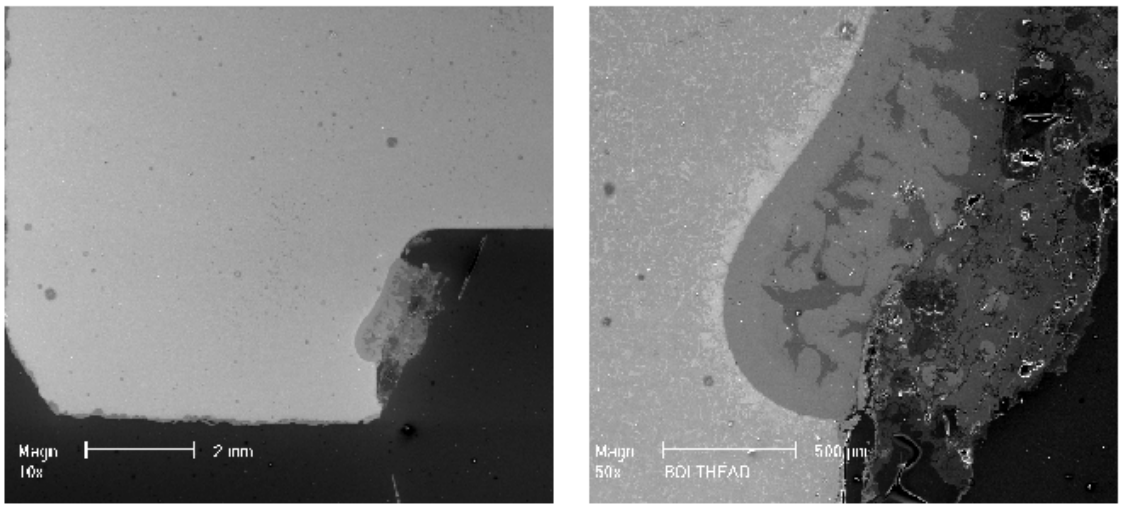

Figure 4-12. (a) Scanning Electron Microscope Secondary Electron Image of Car 52 Air Brake Valve Bolt Head Showing Iron and Aluminum and (b) Closeup of Iron with Aluminum

4.3 Discussion

Analyses of the scale obtained from Car 51 suggest the oxide was initially formed as a result of high-temperature oxidation. Subsequent exposure to water or humid air resulted in the formation of iron hydroxides that are typical of corrosion products for steel structures exposed to a humid or aqueous environment. Calculations of the time and temperature required to form oxide scales of similar in thickness to the specimens obtained from Car 51 or from the roof of Car 50 do not consider changes in thickness that may result from subsequent exposure to humidity or water.

The thickness of the oxide scales recovered from Car 51 and the reduced metal thickness observed in the roof panel of Car 50 correspond to temperatures in the range of 750 to 850°C [1,382 to 1,562 °F]] for a period of approximately 4 hours. The estimation of the temperature does not consider the effects of steel composition and microstructure (Runk and Kim, 1970; Hauffe, 1965) or the partial pressure of oxygen (Kubaschewski and Hopkins, 1962) on the oxidation kinetics. Cross sections of the roof panel from Car 50 clearly indicate significant cracking of the oxide, suggesting the roof panel reached temperatures where spalling of the oxide may be expected. Cracks in the oxide scales tend to increase the oxidation rate of the underlying metal. Assessment of the oxide layer thickness is compromised by scale thickness variation and scale spalling. As a result, assessments of the temperature of the component and fire duration using the thickness of the oxide scales may have significant errors.

Estimations of component temperature and fire duration from the analysis of the oxide scale thickness and the reduction in the metal thickness are dependent on the selection of kinetic parameters. As indicated in Section 4.1, the rate constants are dependent on several factors, including microstructure and composition. Additional calculations were performed to determine the effects of uncertainty in the values of the rate constants. Multiplying the rate constants shown in Figure 4-1 by a factor of 2 increased the oxide scale or reduced metal thickness by approximately 50 percent.

Spalling of the oxide may also be problematic for the assessment of temperature because of uncertainty in the conditions necessary for spalling to occur and the uncertainty in the oxidation rates after spalling of the oxide scale. On the other hand, the adhesion of iron oxides to iron is a function of temperature and scale thickness (Kubaschewski and Hopkins, 1962) and may provide a marker for the temperature achieved by the steel components. For scales of 200 µm [0.0079 in] thickness, the adhesion increases as temperature increases from 650 to 775 °C [1,202 to 1,427 °F] and then decreases to zero at 950 °C [1,742 °F]. When the adhesion strength decreases, the oxide can be easily removed from the metal, and spalling can occur. Spalling of oxide scales on iron and steel is generally observed at temperatures of 850 °C [1,562 °F] but has been observed as low as 700 °C [1,292 °F] (Kubaschewski and Hopkins, 1962). The scale recovered from the brake end of Car 51 adjacent to Car 52 was completely separated from the underlying steel, suggesting the steel reached temperatures above 700 °C [1,292 °F].

The oxide scale on the bolt recovered from the air brake valve of Car 50 appeared to be more intact than the scale on the roof panel of Car 50, suggesting that the oxide on the bolt was formed at a lower temperature. The observation of the aluminum–iron–silicon phase on the underside of the bolt head is inconsistent with the lower component temperature suggested by the intact, 53-µm [0.0021-in] thick oxide scale on the shank of the bolt. It is unlikely that the

formation of aluminum–iron–silicon occurred as a result of diffusion of aluminum into the steel bolt. No low melting point eutectic exists in the aluminum–iron, aluminum–silicon, or the iron–silicon systems that would result in the formation of this phase.

Initial analyses of the sand collected from the tunnel did not provide a means to estimate temperature. Quartz has a melting temperature of 1,610 °C [2,930 °F], which is greater than the solidus temperature of carbon steel. Although not completely conclusive, the x-ray diffraction analyses indicated the presence of ankerite, which contains carbonate. Carbonate minerals tend to decompose and evolve carbon dioxide at elevated temperatures. Specific information on ankerite was not available but ankerite is similar to dolomite [$CaCO_3 \cdot MgCO_3$], which decomposes at temperatures above 730 °C [1,346 °F]. Because ankerite appears to be present in both sand samples collected at locations close to and away from the fire, it appears that the sand collected from Rail #44 did not achieve temperatures in excess of 730 °C [1,346 °F].

5 ALUMINUM SAMPLE THERMAL MODEL

A fundamental heat transfer analysis of the aluminum air brake cover found on Car 51 was conducted. The procedure followed is commonly used to predict the length of exposure required to bring a structural element to a critical temperature and the failure times in steel sections, based on strength reductions at elevated temperatures.

5.1 Assumptions

To simplify our initial analysis, the following assumptions were made:

Lumped Mass—The aluminum components were assumed to be lumped masses of solid aluminum. It is also assumed that the temperature of the relatively small volume of aluminum is uniform. This assumption is conservative because it will over predict the amount of aluminum present for phase change.

Full Volume of Aluminum—In the absence of an accurate values of aluminum volume contained in the valve cover, a calculation of the volume of the cover was made based on dimensions provided in WABTEC drawings. This assumption is conservative because it will predict higher temperatures to cause melting of the larger volume.

Complete Melting—The aluminum section reached its liquidus temperature. This is a good assumption considering the condition of the covers in Figure 3-2.

Zero Conductive Losses to Adjacent Valve—This analysis considers the aluminum portion separate from any adjacent material. This condition will predict slightly faster melting times than the actual case, which is, however, a fair assumption when the cover deforms and drips away from the main valve assembly.

Convective Heat Transfer Coefficient—The heat transfer coefficient was assumed to be 50 kW/m²K. This value was taken from the Eurocode, as referenced in Buchanan (2001). This heat-transfer coefficient is suggested when calculating the exposure of steel elements in a hydrocarbon fire. According to Buchanan, heat transfer is not strongly heat-transfer coefficient dependent because the primary heat-transfer mode is radiation.

Flame Temperature—A common flame temperature for a typical hydrocarbon fuel is between 810 and 925 °C [1,490 and 1,697 °F] (DeHaan, 1991). The analysis utilized two types of ramp functions; ramp to a maximum temperature and plateau; and ramp-plateau-decay temperature profiles. The ramp-plateau decay fire profile most accurately represents the conditions in the tunnel because of the ventilation constraints of the tunnel geometry. Results for ramp-plateau and ramp-plateau-decay functions are presented in Section 5.4.

Radiative Exposure—The added exposure because of radiation from the luminous flame was not considered. The radiative fraction is typically taken to be approximately 30 percent of the total heat release of the burning fuel. This fraction changes with changes in oxygen availability and burning efficiency of the fuel. Appropriate values for radiant exposures range between 20 and 50 kW/m². These values were chosen based on published radiative fractions of known hydrocarbons (Tewarson, 1995; Drysdale, 1985). The exclusion of radiative inputs will lead to longer predicted exposure times.

5.2 Basic Equations

The analysis is based on the principle that heat entering the aluminum section over a period of time (Δt) raises the temperature by some amount (ΔT). This concept is represented as

$$\dot{q}'' \bullet F \Delta t = \rho_{Al} \bullet c_{Al} \bullet V \bullet \Delta T_{Al} \tag{5-2}$$

where

$$\dot{q}'' = h_c\left(T_f - T_{Al}\right) + \sigma \varepsilon \left(T_f^4 - T_{Al}^4\right) \tag{5-3}$$

Substituting Eq. (5-2) into Eq.(5-1) yields:

$$\Delta T_s = \frac{F}{V} \bullet \frac{1}{\rho_s c_s} \left\{ h_c\left(T_f - T_{Al}\right) + \sigma \bullet \varepsilon \left(T_f^4 - T_{Al}^4\right) \right\} \Delta t \tag{5-4}$$

where

ΔT_{Al}	—	Change in aluminum temperature (K)
F	—	Surface area (m²)
V	—	Volume (m³)
ρ	—	Density of aluminum (2,707 kg/m³)
c_{Al}	—	Specific heat of aluminum (0.892 kJ/kgK)
h_c	—	Heat transfer coefficient (50 W/m²K)
T_f	—	Flame temperature (K)
T_{al}	—	Aluminum temperature (K)
σ	—	Stefan-Boltzman constant (56.7×10^{-12} kW/m²K⁴)

Emissivity (ε) is given by

$$\varepsilon = \frac{1}{\left[\left(\frac{1}{\varepsilon_S} + \frac{1}{\varepsilon_R}\right) - 1\right]} \tag{5-5}$$

where

ε_S	—	Emissivity of the source
ε_R	—	Emissivity of the receiver

Emissivities were assumed to be 0.67 for both the emitter and the receiver (Buchanan, 2001).

5.3 Analysis Method

A timestep (Δt) was chosen, and the equations were solved to provide the ΔT at each timestep. A Microsoft® VisualBasic program was used for the repetitive calculations. A brief sensitivity analysis was performed on h_c and ε, because these two variables are easily changed (as opposed to the material property variables).

Two temperature functions were tested, as described in Section 5.1. The analysis focused on ramp-plateau and ramp-plateau-decay temperature profiles. Standard values for nonene (or similar hydrocarbon fuels) indicate a flame temperature between 810 and 925 ˚C [1,697 ˚F]. These values were used as starting points for the thermal analysis. Where possible, data obtained from metallurgical analyses were used to further adjust the temperature profile.

5.4 Results

Preliminary model results for several possible fire scenarios are provided. All the results presented assume the same sample geometry, material properties, and heat transfer coefficients. The constant inputs are provided in Sections 3.1 and 5.1. Fire temperature profiles were varied and predicted aluminum profile performance was noted.

5.4.1 Ramp-Plateau Function

The ramp-plateau function assumed the maximum temperature was realized in 3 minutes, and was maintained for the duration of the exposure. This ramp function is typical of hydrocarbon fires modeled in test furnaces. The American Society for Testing and Materials (1993) suggests a temperature of 1,093 ˚C for 3 minutes and 1,180 ˚C [2,156] for 5 minutes, and all times thereafter. This is a very conservative assumption considering the limited availability of fuel (based on spill rate) and the limited supply of oxygen for combustion (based on tunnel geometry).

When modeled using this fire exposure, the sample aluminum element exhibits melting at 300 seconds into the exposure (see Figure 5-1).

A more realistic ramp function would use the upper and lower bound for flame temperature, as found in the literature. These temperatures are 810 and 925 ˚C [1,490 and 1,697 ˚F], respectively. These exposure conditions predict melting at approximately 500 seconds.

Both of these models predict the aluminum melted before a reasonable fire duration could be obtained.

Figure 5-2 illustrates that, when taking the published flame temperature as the maximum temperature experienced by the valve, any exposure time greater than 360 seconds will produce melting conditions.

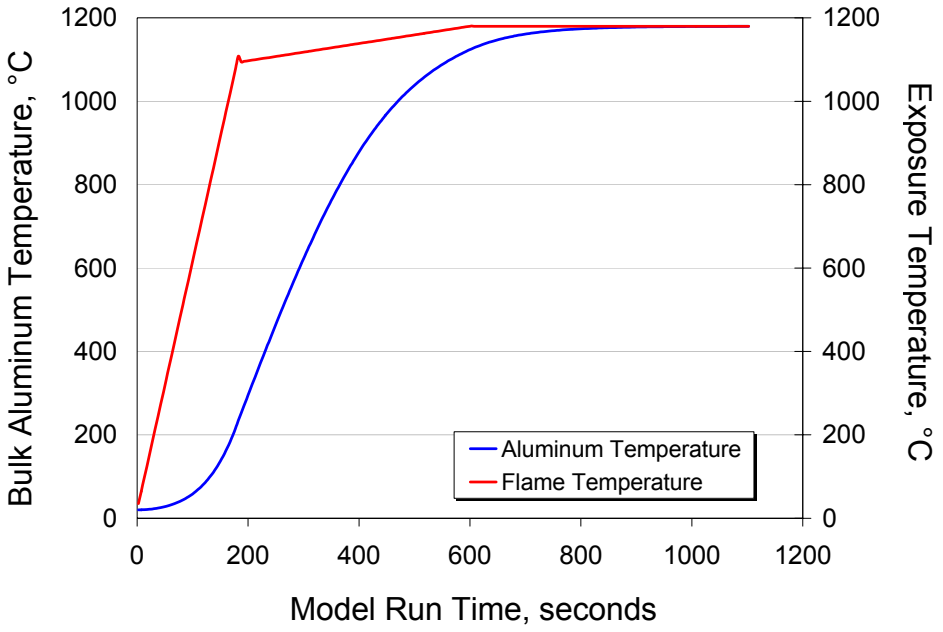

Figure 5-1. ASTM E 1529 (1993) Ramp Function and Corresponding Aluminum Thermal Profile (Melting Predicted at 300 seconds)

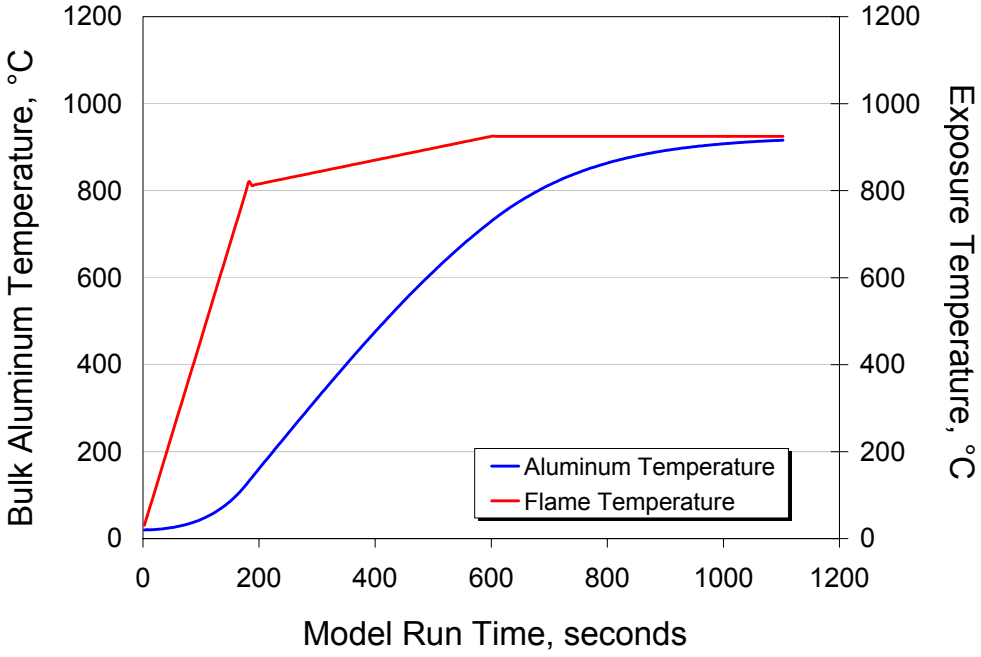

Figure 5-2. Published Flame Temperature Ramp Function and Corresponding Aluminum Thermal Profile (Melting Predicted at ~500 seconds)

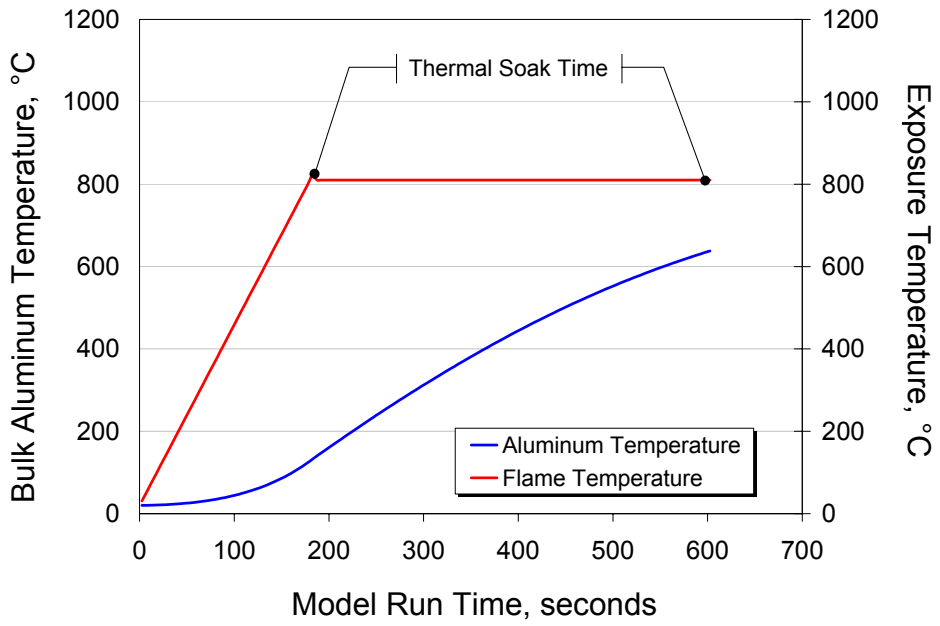

Figure 5-3. Ramp-Plateau Function Demonstrates Melting at Published Flame Temperature for Exposure Times Greater than 360 Seconds

5.4.2 Ramp-Plateau-Decay Function

A more realistic approach is to take into account a slower growth rate and the decay in flame temperature as oxygen becomes scarce in the tunnel. Flammable liquids burning in pool fires, in open air, can be expected to provide temperature profiles consistent with Figures 5-2 and 5-3. Fires burning under limited oxygen conditions will decay following the initial rise and stabilize at some equilibrium temperature until ventilation conditions change or fuel is exhausted. It is also safe to assume the temperatures at the valve {roughly 10 m [33 ft] from the source} would have taken longer to reach the flame temperature. According to ASTM E 1529 (1993), a 3-minute ramp will completely immerse an element in an open-burning fire. A 7.5-minute initial ramp was chosen here. A decay to half the fire temperature was assumed to have occurred 18 minutes into the fire exposure (assuming oxygen starvation).

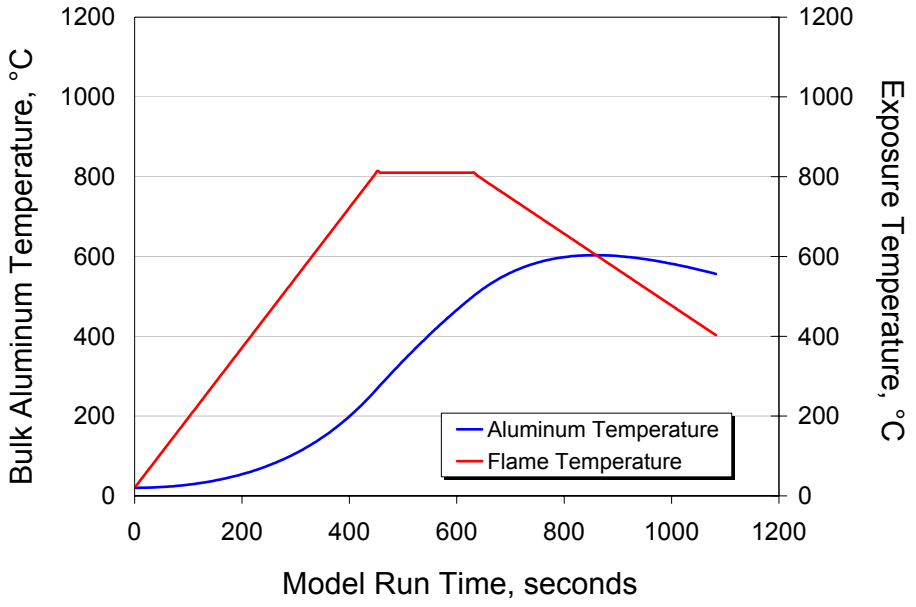

Figure 5-4. Ramp-Plateau-Decay Function and Corresponding Aluminum Thermal Profile (Melting Predicted at ~800 seconds)

The conditions depicted in Figure 5-4 may be more difficult than originally assumed because 810 ˚C [1,490 ˚F] is the actual, published flame temperature of the fuel. The valve would have had to be completely engulfed in flames for it to realize these temperatures. Considering the location of the value, 10 m [33 ft] uphill, and its position in the tunnel (low to the floor), total flame engulfment may have only occurred intermittently and, possibly, for only a short duration.

5.5 Discussion

The model was run with several variations in h_c and ε. In all cases, the model predicted the melting occurred between 793 seconds (assuming h_c = 25 W/m²K and ε = 0.26) and 463 seconds (assuming h_c = 50 W/m²K and ε = 0.5). The predictions of melting at far less than 1,800 seconds could not be used to ascertain the duration of the exposure.

Even when not considering the radiative exposure of the sample to the flame luminosity, the melting time of the valve cover is predicted to have occurred early in the exposure. Considering the radiative inputs would have considerably decreased the melting time. In relation to laboratory testing, in order to simulate a radiative heat flux of 50 kW/m², samples are exposed to a furnace environment of approximately 800 °C [1,472 ˚F].

Had the model predicted melting at over 1,800 seconds, one could deduce the fire duration was at least 1,800 seconds. The data indicated the aluminum section melted very early in the fire duration and the aluminum was severely damaged as a result of the fire exposure before the aluminum performance could be used to establish fire duration.

6 CONCLUSIONS

Metallurgical analyses were conducted to assess the fire temperature and fire duration. The analyses were partially confounded by several factors including the atmospheric exposure of the rail car components for a period of more than 1 year following the fire. Another limitation of the analyses was the lack of suitable controls, or components that were not exposed to the fire, that could be used to assess extent of fire damage to the recovered components. Metallurgical analyses suggest that the fire temperature at the end of Car 51, adjacent to Car 52, was at least 700 ˚C [1,292 ˚F] and likely closer to 850 ˚C [1,562 ˚F], based on the observation of spalling of the oxide scale. Based on the reduction in the thickness of the roof of Car 50, temperatures for this component were estimated to be in the range of 750 to 850 ˚C [1,382 to1,562 ˚F] for a period of 4 hours. The oxide formed on the steel bolt from the air brake valve assembly of Car 52 suggests the temperature in this region was estimated to be 627 ˚C [1,160 ˚F] for an exposure period of 4 hours.

The preliminary data reviewed, including a first-look metallurgical analysis coupled with a simplified thermal model, indicate conditions causing melting in the aluminum could only occur if temperatures in excess of 600 ˚C [1,112 ˚F] were achieved in the sample, for an appreciable duration.

A second aluminum witness was found approximately 20 m [66 ft] uphill of the fire source. This piece is shown in Figure 6-1. It is interesting to note that this piece did not melt completely, which would indicate the very specific conditions required to melt the valve assembly on Car 52 were likely not encountered at approximately 20m [66 ft] away.

Figure 6-1. Air Brake Valve Found 20+ m [66 ft] from Fuel Spill Site (Note Only Partial Melting at This Location)

Closer analysis of the damage caused to the valve cover found at Car 52, indicates that a separation distance of approximately 20 m [66 ft] was sufficient to limit the exposure conditions in this area, as evidenced by the level of damage to the valve cover. Considering only partial

melting in this area, temperatures at the surface of the aluminum were only slightly above 600˚C [1,112˚F] (enough to initiate melting) but were not maintained for any appreciable duration.

A third valve, of similar construction to the valves found on Cars 51 and 52, was also found on Car 53 (approximately 40 m [downhill] from the tripropylene spill point). This valve exhibited no signs of damage at all, and was found completely intact. Thus, at separation distances of 40 m or greater, the exposure conditions were demonstrated to be less than 600˚C.

The exposure profile derived from the post-fire condition of a number of aluminum valve covers is further supported when one considers other damage noted on the railcars. Railcars (e.g. Cars 50 and 51) were painted with Dupont paint No. 909M-22416, an air-dried, high solid, alkyd-enamel paint. Given the observed damage to the steel and paint on Cars 51, 52, and 53, the blistering temperature of 700 ˚C was only realized within 15 m of the spill site. These distances were measured from the tops of the railcars (worst case), where both heat and corrosive products of combustion were concentrated. There was no damage to the paint or steel on Car 53, adjacent to the fuel spill car (52), and located 12 m from the spill site.

The exposure conditions of standard compliance tests are based on a diesel, or similar hydrocarbon, pool fire burning in an open pool configuration. For testing purposes, this fire scenario provides exposure temperatures of approximately 800 ˚C [1,472 ˚F] for 30 minutes. It is also assumed in this scenario the item being tested is in close proximity to the fuel spill source and is completely immersed in the fire environment. Administrative controls can ensure conditions that would limit the proximity of fuel sources to important cargo. The data obtained during this review of the Baltimore Tunnel Fire indicate the separation of cargo from potential fuel sources will be an acceptable method of limiting their exposure.

7 REFERENCES

ASM International. *ASM Handbook Volume 3: Alloy Phase Diagrams.* Materials Park, Ohio: ASM International. 1992.

ASTM. "Standard Test Methods for Determining Effects of Large Hydrocarbon Pool Fires on Structural Member and Assemblies." ASTM E 1529–93. 1993.

Buchanan, A.H. *Structural Design for Fire Safety.* West Sussex, England: John Wiley and Sons, Limited. 2001.

DeHaan, J.D. *Kirk's Fire Investigation—3rd Edition.* Englewood Cliffs, New Jersey: Brady—A Prentice Hall Division. 1991.

Drysdale, D. An Introduction to Fire Dynamics. New York City, New York: John Wiley and Sons, Limited. 1985

Geiger, G.H. and D.R. Poirier. *Transport Phenomena in Metallurgy.* Reading, Massachusetts Addison-Wesley Publishing Company. 1980.

Hauffe, K. *Oxidation of Metals.* New York City, New York: Plenum Press. 1965

Holman, J.P. *Heat Transfer—7th Edition.* New York City, New York: McGraw-Hill, Inc. 1990.

Kubaschewski, O. and B.E. Hopkins. *Oxidation of Metals and Alloys.* New York City, New York: Academic Press Inc. 1962.

Larose, S. and R.A. Rapp. "Review of Low Temperature Oxidation of Carbon Steels and Low Alloy Steels for Use as High-Level Radioactive Waste Package Materials." CNWRA 97-003. San Antonio, Texas: Center for Nuclear Waste Regulatory Analyses. 1997.

Rapp, R.A. *High Temperature Corrosion* (Reference Manual for Audio Course). Washington, DC: The American Chemical Society. 1980.

Runk R.B. and H.J. Kim. "The Oxidation of Iron-Carbon Alloys at Low Temperatures." *Oxidation of Metals.* Vol. 2, No. 3. p. 285. 1970.

Simms, N.J. and J.A. Little. "High-Temperature Oxidation of Fe-$2^1/_4$Cr-1Mo in Oxygen." *Oxidation of Metals.* Vol. 27, Nos. 5/6. p. 283. 1987.

Szlarska-Smialowska Z. and J. Jurek. "Ellipsometric Studies on Iron Oxide Film Growth at 100–350 °C." *Corrosion.* Vol. 32, No. 7. p. 294. 1976.

Tewarson, A. *Generation of Heat and Chemical Compounds in Fires—Society of Fire Protection Engineers (SFPE) Handbook.* Section 3, Chapter 4. pp. 3-99–100. Quincy, Massachusetts: National Fire Protection Association. 1995.